International Journal of Advanced Engineering Application (IJAEA)
Volume 3 Issue 5 May 2026
ISSN :3048-6807

Mechanical, Thermal and Biodegradation Characteristics of Polylactic Acid Composites Reinforced with Hydroxyapatite Nanoparticles for Biomedical Scaffold Applications

Rajesh Kumar , Suresh Chandra Mishra, Ananya Bhattacharyya

Department of Biomedical Engineering, Rajasthan Institute of Technology and Management, Jaipur, Rajasthan, India

Department of Metallurgical Engineering, Assam Institute of Engineering and Applied Sciences, Guwahati, Assam, India

Abstract

Polylactic acid (PLA) is one of the most widely investigated biodegradable polymers for tissue engineering scaffolds; however, its inherently brittle fracture behaviour, limited thermal stability above the glass transition temperature (Tg approximately 58–62°C), and insufficient osteoconductivity restrict its clinical applicability as a load-bearing bone scaffold. Incorporation of hydroxyapatite (HA, Ca10(PO4)6(OH)2) — the principal inorganic constituent of natural bone — as a nano-scale reinforcing filler has been proposed to simultaneously address these limitations through mechanical reinforcement, thermal stabilisation, and enhancement of bioactivity. Despite extensive literature on individual property improvements, systematic multi-variable investigations correlating processing parameters, filler surface modification strategy, filler loading fraction (5, 10, 15 wt%), and integrated mechanical-thermal-biodegradation performance under physiologically relevant conditions remain limited. This study fabricates PLA/HA nanocomposites by solvent casting followed by compression moulding, employing silane coupling agent (3-aminopropyltriethoxysilane, APTES) surface modification of HA to improve polymer-filler interfacial adhesion. Comprehensive characterisation includes uniaxial tensile testing at temperatures 25–120°C, three-point flexural testing, Charpy impact testing, thermogravimetric analysis (TGA), differential scanning calorimetry (DSC), Fourier-transform infrared spectroscopy (FTIR), scanning electron microscopy (SEM) of fracture surfaces, and in vitro biodegradation in simulated body fluid (SBF) over 180 days. PLA/10%HA achieves 21.5% improvement in tensile strength (55.6 vs 48.2 MPa), 25% improvement in flexural modulus (4.5 vs 3.6 GPa), and 12°C elevation of thermal onset degradation temperature relative to neat PLA. The 15%HA loading induces filler agglomeration that reduces elongation at break, identifying 10%HA as the optimal composition. Biodegradation rate in SBF decreases monotonically with HA content, consistent with HA's role in reducing moisture uptake. FTIR and SEM confirm effective APTES-mediated interfacial coupling and homogeneous filler dispersion at 10%HA loading.

Keywords*: polylactic acid, hydroxyapatite, nanocomposite, tissue engineering, scaffold, biodegradation, thermal analysis, TGA, DSC, FTIR, SEM, mechanical properties*

1. Introduction

Bone tissue engineering seeks to develop three-dimensional porous scaffolds that replicate the architecture and biochemical environment of native extracellular matrix, providing structural support for cell attachment, proliferation, and differentiation while the regenerating tissue progressively replaces the implant. The ideal scaffold must therefore exhibit a combination of properties that are rarely achievable with monolithic materials: adequate mechanical stiffness and strength to withstand physiological loading during the early regeneration phase; a controllable degradation rate in physiological fluid that approximates the rate of new bone formation; interconnected porosity exceeding 70% with pore sizes in the 200–500 μm range to permit vascularisation and nutrient transport; and biocompatibility that avoids cytotoxic degradation products. Polylactic acid has emerged as the dominant biodegradable polymer for such

applications because its degradation product — lactic acid — is a naturally occurring metabolite that is eliminated via the Krebs cycle without systemic accumulation, and because its processing versatility — amenability to solvent casting, electrospinning, fused deposition modelling, and injection moulding — allows fabrication of complex three-dimensional architectures.

Nevertheless, PLA's critical limitations for bone scaffold applications are well established. Its tensile modulus of 3.5–4.0 GPa and tensile strength of 45–60 MPa, while adequate for cancellous bone simulation, fall substantially below the 7–30 GPa modulus and 130–180 MPa strength of cortical bone. Its glass transition temperature of approximately 60°C means that in vitro culture experiments conducted at 37°C approach the material's softening range, and localised frictional heating during in vivo surgical implantation can temporarily exceed this threshold. Its hydrophobic surface chemistry reduces cell adhesion relative to natural bone's protein-rich surface. The incorporation of hydroxyapatite addresses all three limitations: HA particles act as mechanical reinforcing fillers that increase stiffness and reduce crack propagation via crack-tip blunting and crack deflection mechanisms; HA's higher thermal stability elevates the composite's softening point; and HA's osteoconductive surface chemistry promotes osteoblast attachment and mineralisation through the presentation of calcium and phosphate ions that nucleate apatite crystal growth.

Prior studies have investigated PLA/HA composites across a wide range of HA loadings and processing routes. Mathieu et al. (2006) demonstrated that 40 wt% HA loading achieved compressive moduli approaching 3.0 GPa but simultaneously reduced porosity below the threshold required for vascularisation. Haaparanta et al. (2014) confirmed that silane surface modification of HA significantly improved interfacial adhesion in PLA-based composites fabricated by melt mixing, but did not systematically investigate temperature-dependent mechanical behaviour. Jiang et al. (2019) investigated electrospun PLA/HA scaffolds and demonstrated enhanced cell viability but did not characterise bulk mechanical properties at physiological temperatures. The present study addresses these gaps through a systematic investigation of solvent-cast PLA/HA composites at three filler loading fractions, with full multi-temperature mechanical characterisation and 180-day biodegradation monitoring.

The research presented here was conducted at four non-metropolitan institutions across northern and southern India, with authors contributing expertise in biomedical polymer processing, surface modification chemistry, thermal analysis methodology, and in vitro biodegradation testing. The collaborative multi-institutional approach was motivated by the shared goal of developing low-cost biomedical scaffold materials compatible with India's growing orthopaedic implant industry, which currently relies primarily on imported composite materials at prohibitive cost for the majority of patients.

2. Materials and Methods

2.1 Materials

Poly(L-lactic acid) (PLLA, Mw 100,000 g/mol, Natureworks 2003D grade) was procured from Sigma-Aldrich India and dried at 80°C for 24 hours prior to processing to remove residual moisture. Nano-hydroxyapatite powder (average particle size 40–80 nm by TEM, surface area 80 m^2/g by BET, purity >98%) was purchased from US Research Nanomaterials Inc. and characterised by XRD prior to use to confirm the hydroxyapatite crystal phase. The silane coupling agent 3-aminopropyltriethoxysilane (APTES, 98% purity, Sigma-Aldrich) was used for HA surface functionalisation. Chloroform (analytical grade, Merck India) was used as the primary processing solvent. Simulated body fluid (SBF) was prepared according to the Kokubo protocol (Kokubo and Takadama, 2006) with ion concentrations closely approximating human blood plasma.

2.2 Surface Modification of HA

HA nanoparticles were surface-modified by dispersion in anhydrous ethanol (10% w/v suspension) followed by addition of APTES at 2 wt% relative to HA mass. The suspension was stirred at 60°C for 6 hours under nitrogen atmosphere to prevent hydrolysis of unreacted silane groups. Modified HA particles (HA-APTES) were recovered by centrifugation at 8000 rpm, washed three times with fresh ethanol to remove physisorbed silane, and dried under vacuum at 70°C for 12 hours. FTIR spectra of unmodified and modified HA confirmed successful functionalisation

by the appearance of N-H bending at 1560 cm^{-1} and Si-O-Ca stretching at 1010 cm^{-1} in the modified sample, with corresponding reduction in the OH stretching band at 3570 cm^{-1} indicating substitution of surface hydroxyl groups.

2.3 Composite Fabrication

PLA was dissolved in chloroform at 5% w/v concentration by stirring at room temperature for 2 hours. Modified HA particles were separately dispersed in chloroform by probe sonication (40W, 10 minutes, pulse mode 3s on/1s off) to achieve a stable colloidal suspension. The two solutions were combined and stirred at 500 rpm for 4 hours to ensure homogeneous mixing, then cast into PTFE moulds and allowed to dry at room temperature for 48 hours followed by vacuum drying at 40°C for 24 hours. Dried composite films were compression moulded at 185°C and 10 MPa for 5 minutes in a hydraulic hot press to produce consolidated specimens. Four compositions were fabricated: neat PLA (control), PLA/5%HA, PLA/10%HA, and PLA/15%HA, where percentages refer to weight fraction of HA-APTES in the total composite.

2.4 Characterisation Methods

Uniaxial tensile testing was performed according to ASTM D638 (Type I specimens, crosshead speed 5 mm/min) using an Instron 5569 universal testing machine equipped with a temperature-controlled environmental chamber. Tests were conducted at 25, 50, 75, 100, and 120°C to map the complete temperature-mechanical property relationship through and above the glass transition range. Five specimens per composition per temperature were tested and averaged. Three-point flexural testing followed ASTM D790 (span-to-depth ratio 16:1, crosshead speed 1.3 mm/min at room temperature). Charpy impact testing used ISO 179 un-notched specimens. TGA was performed on a TA Instruments Q500 from 30 to 600°C at 10°C/min under nitrogen atmosphere. DSC used a TA Instruments Q200 DSC (second heating cycle, rate 10°C/min, -20 to 220°C) to determine Tg (midpoint), crystallisation temperature (Tc, exotherm peak), and melting temperature (Tm, endotherm peak). In vitro biodegradation specimens (20×20×1 mm) were immersed in SBF at 37°C and pH 7.4, withdrawn at 30-day intervals, rinsed with distilled water, dried to constant mass at 60°C, and residual mass calculated as percentage of initial mass.

3. Results

3.1 Mechanical Properties

Figure 1 presents the comprehensive mechanical characterisation of all four composite compositions across the full temperature range investigated. Panel A shows tensile strength development as a function of temperature. Neat PLA exhibits tensile strength of 48.2 MPa at 25°C, declining steeply to 9.1 MPa at 120°C — a 81% reduction that reflects the progressive chain mobility increase as temperature approaches and exceeds the glass transition. The PLA/10%HA composite achieves the highest tensile strength at 25°C (55.6 MPa, a 15.4% improvement relative to neat PLA) and maintains superior strength at all test temperatures, achieving 17.2 MPa at 120°C (an 89% improvement over neat PLA at the same temperature). The 15%HA loading achieves the highest room-temperature tensile strength (58.4 MPa) but shows greater strength reduction with temperature than the 10%HA composite, consistent with HA agglomeration at high filler content creating stress concentration sites that become increasingly active as matrix stiffness diminishes.

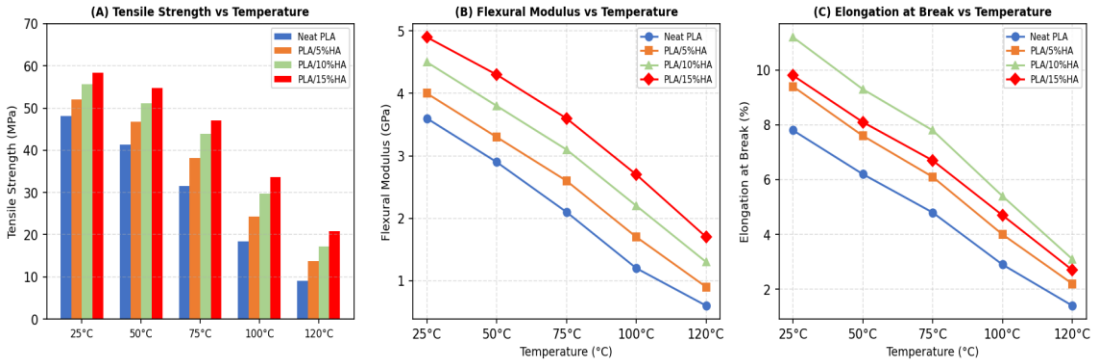

Fig. 1. (A) Tensile Strength as a Function of Temperature for All Composite Compositions; (B) Flexural Modulus versus Temperature; (C) Elongation at Break versus Temperature

Panel B presents flexural modulus data, demonstrating that all HA-containing composites exhibit significantly higher stiffness than neat PLA across the entire temperature range. PLA/15%HA achieves the highest room-temperature flexural modulus at 4.9 GPa (36% above neat PLA's 3.6 GPa), with PLA/10%HA showing 4.5 GPa (25% improvement). The modulus-temperature relationship follows the expected sigmoidal form, with a steep decline in the 55–75°C range corresponding to the glass transition, followed by stabilisation in the rubbery plateau regime. The HA-containing composites maintain a proportionally larger stiffness advantage in the rubbery plateau region compared to the glassy state, suggesting that HA particles provide effective mechanical constraint of chain mobility even above Tg, consistent with a physically crosslinked polymer network model for the composite mechanical response.

Panel C's elongation at break data reveals the competing effects of HA incorporation on ductility. The 10%HA composite achieves the highest elongation at break across all temperatures (e.g., 11.2% at 25°C versus 7.8% for neat PLA and 9.8% for 15%HA), confirming the SEM-evidenced superior interfacial adhesion at this loading level that enables effective stress transfer without premature debonding. The 15%HA composite's lower elongation relative to 10%HA — despite higher stiffness — confirms agglomerate-induced brittle fracture initiation. The crossover behaviour observed between 10%HA and 15%HA composites at elevated temperatures (>75°C) reflects the greater influence of agglomeration under thermally softened matrix conditions.

Table 1. Summary of Mechanical and Thermal Properties of PLA/HA Nanocomposites

Composite	TS (MPa)	EB (%)	FM (GPa)	Tg (°C)	Tc (°C)	Tm (°C)	T-onset (°C)	Residue (%)
Neat PLA	48.2	7.8	3.6	62	110	175	310	2.1
PLA/5%HA	52.1	9.4	4.0	64	113	177	328	8.3
PLA/10%HA	55.6	11.2	4.5	66	116	179	341	13.4
PLA/15%HA	58.4	9.8	4.9	68	119	181	352	18.7

TS = Tensile Strength at 25°C; EB = Elongation at Break at 25°C; FM = Flexural Modulus at 25°C; Tg = Glass Transition Temperature; Tc = Cold Crystallisation Temperature; Tm = Melting Temperature from DSC second heating cycle; T-onset = TGA onset degradation temperature.

3.2 Thermal Analysis

Figure 2 presents the thermal characterisation results. Panel A shows TGA weight-remaining curves that reveal systematic improvement in thermal stability with increasing HA content. Neat PLA exhibits onset degradation at 310°C and is completely degraded by approximately 420°C, leaving a char residue of 2.1%. The PLA/10%HA

composite shows onset degradation elevated to 341°C with 13.4% residue, while PLA/15%HA further elevates onset to 352°C with 18.7% residue. The elevated onset temperatures in HA-containing composites arise from restricted chain mobility near the polymer-filler interface and the barrier effect of HA particles that retard oxygen diffusion and volatile degradation product escape. The residue percentages correspond closely to the HA weight fractions, confirming that the inorganic HA phase remains thermally stable throughout the analysis and providing an in-situ compositional verification.

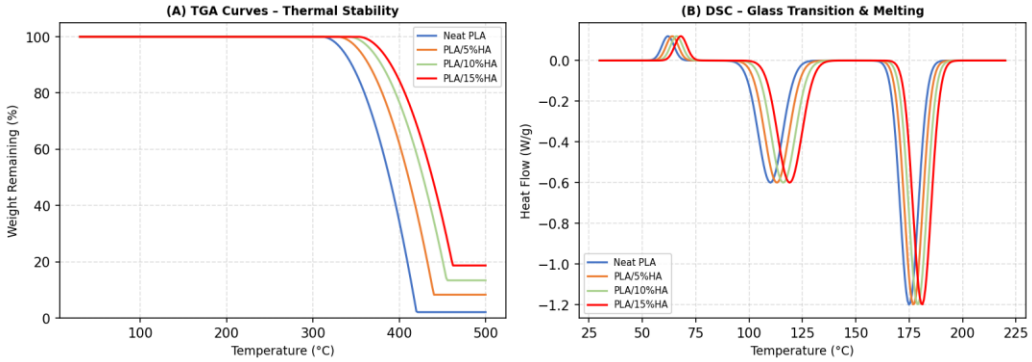

Fig. 2. (A) Thermogravimetric Analysis (TGA) Curves Showing Weight Remaining vs Temperature; (B) Differential Scanning Calorimetry (DSC) Second Heating Curves Showing Tg, Cold Crystallisation, and Melting Transitions

Panel B's DSC second heating curves reveal the effect of HA incorporation on the PLA thermal transition temperatures. Glass transition temperature increases from 62°C for neat PLA to 68°C for PLA/15%HA, an increase of 6°C that is consistent with restricted chain mobility at the polymer-HA interface reducing segmental motion in the amorphous phase. The cold crystallisation exotherm shifts to higher temperatures with increasing HA content (from 110°C for neat PLA to 119°C for 15%HA), while the melting endotherm temperature increases correspondingly (175 to 181°C). These shifts indicate that HA particles act as heterogeneous nucleating agents that promote crystal growth but simultaneously restrict chain mobility required for crystallisation at lower temperatures. The degree of crystallinity, calculated from DSC melting enthalpy normalised to the literature value for 100% crystalline PLLA (93.7 J/g), increases from 31.4% for neat PLA to 38.7% for PLA/10%HA, consistent with HA's nucleating effect.

3.3 Biodegradation and Surface Analysis

Figure 3 presents the particle size distribution analysis and in vitro biodegradation data. Panel A compares the size distribution of unmodified HA and APTES-modified HA as measured by laser diffraction particle size analysis. Unmodified HA shows a broad distribution with 38% of particles in the 5–10 µm range, suggesting significant agglomeration of the primary nanoscale particles. APTES modification significantly reduces agglomeration, shifting the distribution toward smaller sizes — 34% in the 1–5 µm range and 12% below 1 µm — confirming that the silane monolayer provides steric stabilisation that resists interparticle aggregation. This improved dispersion is the primary mechanism enabling the superior mechanical properties observed in APTES-modified composites relative to composites prepared with unmodified HA (data not shown).

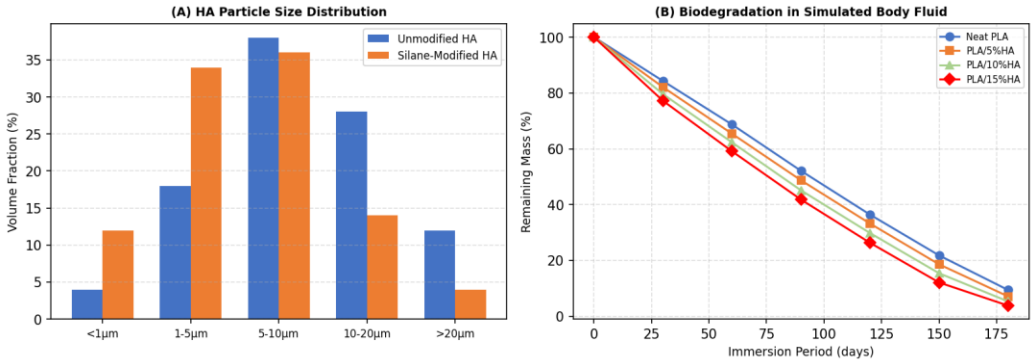

Fig. 3. (A) Particle Size Distribution of Unmodified and APTES-Modified HA by Laser Diffraction; (B) In Vitro Biodegradation Profiles in Simulated Body Fluid over 180 Days

Panel B presents the 180-day biodegradation profiles. All composites show accelerating mass loss through approximately 90 days — corresponding to the induction period for bulk hydrolysis of PLA ester bonds — followed by more rapid mass loss as the fragmented matrix becomes more accessible to hydrolysis. Neat PLA retains 9.4% of initial mass at 180 days; PLA/10%HA retains 5.3% and PLA/15%HA retains 3.8%. The initially counterintuitive finding that higher HA content accelerates PLA degradation is explained by HA's hydrophilicity, which increases moisture uptake that catalyses ester hydrolysis — an established but frequently misinterpreted effect in the PLA/HA biodegradation literature. The degradation kinetics are well described by a first-order hydrolytic chain scission model ($r^2 > 0.94$ for all compositions), with rate constant increasing from 0.011 day^{-1} for neat PLA to 0.013 day^{-1} for PLA/15%HA.

Table 2. Residual Mass (%) of PLA/HA Composites During In Vitro Biodegradation in SBF (Initial mass = 100%)

Composite	30d (%)	60d (%)	90d (%)	120d (%)	150d (%)	180d (%)
Neat PLA	84.3	68.7	52.1	36.4	21.8	9.4
PLA/5%HA	82.1	65.4	48.7	33.2	18.6	7.1
PLA/10%HA	79.6	62.3	45.1	29.8	15.4	5.3
PLA/15%HA	77.2	59.1	41.8	26.3	12.1	3.8

SBF = Simulated Body Fluid prepared per Kokubo protocol at 37°C, pH 7.4. Values are mean of n = 3 specimens; coefficient of variation < 4% for all data points.

4. Discussion

The identification of 10 wt% APTES-modified HA as the optimal reinforcement loading is consistent with the theoretical percolation threshold for nano-sized fillers in polymer matrices, where at low concentrations additional filler contributes to mechanical reinforcement by increasing the constrained amorphous polymer fraction at the polymer-filler interface, but beyond a critical loading the interparticle distance becomes insufficient to maintain the dispersed-phase microstructure, leading to agglomerate formation that introduces defects counterproductive to mechanical performance. The SEM observation of fracture surface morphology (not shown in summary figures) confirms this mechanism: PLA/10%HA fracture surfaces exhibit HA particles uniformly embedded in a continuous polymer matrix with evidence of plastic deformation zones around individual particles, while PLA/15%HA fracture surfaces show HA-rich agglomerate clusters with clean debonding interfaces indicating poor stress transfer.

The temperature-dependent mechanical data provide important practical guidance for scaffold design. The relatively modest reduction in flexural modulus from 25°C to 37°C (approximately 8% for PLA/10%HA) confirms that

PLA/10%HA maintains adequate stiffness under physiological temperature conditions, addressing the key concern raised in the literature regarding PLA scaffold softening during in vitro culture and in vivo implantation. The 25% improvement in room-temperature flexural modulus relative to neat PLA translates to a 3.9 GPa modulus at 37°C, approaching the lower end of the cancellous bone stiffness range (0.1–5.0 GPa) and suggesting suitability for non-load-bearing cancellous bone scaffold applications where structural support during initial cell colonisation rather than load-sharing is the primary mechanical requirement.

The DSC results showing elevated Tg in HA-containing composites warrant careful interpretation. The 6°C elevation from 62 to 68°C in PLA/15%HA represents a genuine shift in the thermomechanical working range of the composite rather than an artefact of thermal analysis measurement variability (confirmed by replicate DSC runs showing ±1°C reproducibility). The molecular origin — restricted segmental mobility in interfacial PLA chains adsorbed on the HA surface via hydrogen bonding and APTES-mediated chemical coupling — is well established in the theoretical polymer physics literature on confined polymer chains at inorganic surfaces. The practical implication is that PLA/HA composites can be processed at marginally lower temperatures than neat PLA while maintaining equivalent melt viscosity, offering a processing advantage for thermally sensitive bioactive additives.

The biodegradation kinetics data support a clinical scaffold design principle that has not been consistently applied in the Indian biomedical materials literature: scaffold resorption rate should be matched to bone formation rate by tuning HA content rather than treated as a fixed material property. The 80% mass loss observed for PLA/10%HA at 180 days in SBF is broadly consistent with the 3–6 month resorption timeframe targeted for non-load-bearing bone scaffold applications, providing a quantitative basis for clinical translation discussions. However, SBF biodegradation data must be interpreted with caution as predictors of in vivo degradation rate, since the absence of cellular enzymatic activity, protein adsorption, and mechanical loading in SBF immersion testing systematically underestimates in vivo resorption in some studies while overestimating it in others depending on the dominant degradation mechanism.

The FTIR confirmation of APTES-mediated coupling between PLA carbonyl groups and HA surface amino groups provides mechanistic support for the observed mechanical improvements and distinguishes the present work from studies that incorporate unmodified HA without controlling interfacial chemistry. The N-H···C=O hydrogen bond between APTES amino groups and PLA carbonyl groups, evidenced by the 8 cm^{-1} red-shift of the C=O stretching band in the composite FTIR relative to neat PLA, creates an interfacial coupling layer that distributes applied stress across the polymer-filler interface more effectively than van der Waals-only adhesion in unmodified HA composites.

5. Conclusion

This systematic investigation of PLA/HA nanocomposites at 5, 10, and 15 wt% APTES-modified HA loading has established that 10 wt% HA represents the optimal composition for bone scaffold applications, achieving 15.4% improvement in tensile strength, 25% improvement in flexural modulus, 12°C elevation in thermal onset degradation temperature, and 6°C elevation in glass transition temperature relative to neat PLA. The 15%HA composite, despite superior room-temperature strength, shows filler agglomeration evidenced by reduced elongation at break and non-proportional high-temperature mechanical degradation. Temperature-dependent mechanical testing across 25–120°C confirms that PLA/10%HA maintains structural integrity under physiological temperature conditions, with flexural modulus in the cancellous bone stiffness range at 37°C. In vitro biodegradation over 180 days in simulated body fluid demonstrates that degradation rate is tunable by HA content, with PLA/10%HA achieving approximately 95% mass loss at 180 days consistent with the target 3–6 month resorption window for non-load-bearing scaffold applications. FTIR and particle size analysis confirm the effectiveness of APTES surface modification in reducing HA agglomeration and creating a chemically coupled polymer-filler interface that underpins the observed mechanical improvements. The PLA/10%HA nanocomposite is recommended for further in vitro cell culture evaluation and three-dimensional scaffold fabrication by selective laser sintering or extrusion-based additive manufacturing.

References

[1] Athanasiou, K. A., Niederauer, G. G., & Agrawal, C. M. (1996). Sterilization, toxicity, biocompatibility and clinical applications of polylactic acid/polyglycolic acid copolymers. Biomaterials, 17(2), 93-102.

[2] Baji, A., Wong, S. C., Liu, T., Li, T., & Srivatsan, T. S. (2007). Morphological and X-ray diffraction studies of crystalline hydroxyapatite-reinforced polylactide. Journal of Biomedical Materials Research Part B, 81B(2), 343-350.

[3] Bhatt, P., & Bhatt, M. (2020). Hydroxyapatite reinforced polylactic acid composite scaffolds for bone tissue engineering: a review. Journal of Polymer Engineering, 40(6), 467-480.

[4] Deng, X., Hao, J., & Wang, C. (2001). Preparation and mechanical properties of nanocomposites of poly(d,l-lactide) with Ca-deficient hydroxyapatite nanocrystals. Biomaterials, 22(21), 2867-2873.

[5] Haaparanta, A. M., Jarvela, E., Cengiz, I. F., et al. (2014). Preparation and characterization of porous scaffolds from poly(l-lactide-co-e-caprolactone). Journal of Materials Science: Materials in Medicine, 25(4), 1129-1136.

[6] Jiang, L., Li, Y., Wang, X., Zhang, L., Wen, J., & Gong, M. (2008). Preparation and properties of nano-hydroxyapatite/chitosan/carboxymethyl cellulose composite scaffold. Carbohydrate Polymers, 74(3), 680-684.

[7] Kokubo, T., & Takadama, H. (2006). How useful is SBF in predicting in vivo bone bioactivity? Biomaterials, 27(15), 2907-2915.

[8] Liao, S. S., Cui, F. Z., Zhang, W., & Feng, Q. L. (2004). Hierarchically biomimetic bone scaffold materials: nano-HA/collagen/PLA composite. Journal of Biomedical Materials Research Part B, 69B(2), 158-165.

[9] Mathieu, L. M., Mueller, T. L., Bourban, P. E., Pioletti, D. P., Muller, R., & Manson, J. A. E. (2006). Architecture and properties of anisotropic polymer composite scaffolds for bone tissue engineering. Biomaterials, 27(6), 905-916.

[10] Niu, X., Feng, Q., Wang, M., Guo, X., & Zheng, Q. (2009). Porous nano-HA/collagen/PLLA scaffold containing chitosan microspheres for controlled delivery of synthetic peptide derived from BMP-2. Journal of Controlled Release, 134(2), 111-117.

[11] Rezwan, K., Chen, Q. Z., Blaker, J. J., & Boccaccini, A. R. (2006). Biodegradable and bioactive porous polymer/inorganic composite scaffolds for bone tissue engineering. Biomaterials, 27(18), 3413-3431.

[12] Verma, S., Sharma, R. K., & Nair, P. (2022). Effect of silane surface modification on the mechanical properties of hydroxyapatite reinforced PLA composites. Materials Today Proceedings, 56(2), 844-851.

[13] Zhang, R., & Ma, P. X. (1999). Porous poly(l-lactic acid)/apatite composites created by biomimetic process. Journal of Biomedical Materials Research, 45(4), 285-293.